Materials Chemistry and Physics 287 (2022) 126320

Contents lists available at ScienceDirect

Materials Chemistry and Physics

journal homepage: www.elsevier.com/locate/matchemphys

Room temperature ferromagnetism in oxygen-deficient gallium oxide films with cubic spinel structure

A. Pichorim [a,*], I.T. Neckel [b], A.J.A. de Oliveira [c], J. Varalda [d], D.H. Mosca [a,d]

[a] Programa de Pós-Graduação Em Engenharia e Ciência Dos Materiais, Universidade Federal Do Paraná – Centro Politécnico, Caixa Postal 19011, 81531-980, Curitiba, Paraná, Brazil
[b] Laboratório Nacional de Luz Síncrotron (LNLS), Centro Nacional de Pesquisa Em Energia e Materiais (CNPEM), 13083-970, Campinas, São Paulo, Brazil
[c] Departamento de Física, Universidade Federal de São Carlos, Rod. Washington Luiz, Km 235 - SP-310, 13565-905, São Carlos, São Paulo, Brazil
[d] Departamento de Física, Universidade Federal Do Paraná – Centro Politécnico, Caixa Postal 19044, 81531-980, Curitiba, Paraná, Brazil

ARTICLE INFO

Keywords:
Room-temperature ferromagnetism
Gallium oxide
Oxygen vacancies
Cubic-spinel structure

ABSTRACT

Oxygen-defective gallium oxide (Ga_2O_{3-x} with $0.4 < x < 0.7$) thin films with cubic spinel structure were deposited on c-cut epi-polished sapphire wafers using thermal evaporation technique by keeping specific values of oxygen partial pressure in the evaporation chamber. The preparation method and post-treatment conditions induced distinct oxygen stoichiometries in the films which exhibit a ferromagnetic-like behavior at room temperature. Despite the measured saturation magnetization values do not exhibit a straightforward correlation to the oxygen stoichiometry of the films, the presence of oxygen vacancies and defects is presumably the origin of the unconventional magnetic behavior. Strong magnetic irreversibility exhibit by the magnetization measurements performed using field-cooling and zero-field-cooling protocols indicate the presence of disordered magnetic moment distributions which are likely non-collinear. Theoretical and experimental results available in the literature corroborate with the assumptions that oxygen vacancies and defects appear as the main reason for room-temperature ferromagnetism. All films exhibit soft magnetic behavior at room temperature, exhibiting remanent magnetizations between 7% and 20% of the saturation magnetization which saturated magnetic moments is estimated as 0.43 and 1.24 Bohr magneton per oxygen vacancy. The present results extend the functionalities of this interesting material, which is already investigated for applications in several technological areas, for possible uses in the areas of spintronics and emerging areas of the optospintronics.

1. Introduction

Gallium oxide (Ga_2O_3) is a material that exhibits six polymorphs [1]. Among them, β-phase is the thermally stable phase since other polymorphs commonly have their average domain size gradually reduced and turning into monoclinic β-Ga_2O_3 with an increase in annealing temperature [2,3]. A special focus is given on potential applications of stable polymorph β-Ga_2O_3 exhibiting wide-bandgap with a direct energy band 4.3–5.3 eV suitable for high-power and high-voltage electronic devices and ultraviolet light emitters [1,4]. However, the phase-dependent photocatalytic activity of Ga_2O_3 varieties in which intrinsic or native defects are found is also intensively studied and discussed because they offer several application opportunities in gas sensing and photocatalytic industrial processes. Particularly, γ-Ga_2O_3 polymorphism with the lowest formation energy [5] when prepared as layered structures with a high concentration of the oxygen vacancies confined in the ultrathin nanosheets exhibit a significant enhancement in the photocatalytic performance, enabling application in several industrial processes and environmental chemistry [6–8]. It is also worth noting that γ-Ga_2O_3 show size-tunable photoluminescence in the visible blue-green regions in quantum dots [6,9,10] and nanorods [11]. Remarkable changes in photoluminescence intensity of γ-Ga_2O_3 nanocrystals, which are synthesized for the same amounts at different times in pure argon, indicate the key role of the concentration of oxygen vacancies [12]. Time-resolved photoluminescence measurements have been shown that photocatalytic activity upon annealing is directly correlated with the native defects (i.e., oxygen vacancy) concentration [13]. These studies also indicate that trapped charge carriers in defect-induced states in γ-Ga_2O_3 nanocrystals unambiguously exhibit a much longer lifetime than those found in surface states, making the

* Corresponding author.
E-mail address: pichorim.andreia@gmail.com (A. Pichorim).

https://doi.org/10.1016/j.matchemphys.2022.126320
Received 28 January 2022; Accepted 25 May 2022
Available online 28 May 2022

charge transfer the main responsible for photocatalytic activity more efficient.

Metastable γ-Ga_2O_3 has a defective spinel-type structure (Space Group number 227) which is like γ-phase Al_2O_3, with Ga^{3+} ions occupying the octahedral (O) and tetrahedral (T) sites which ratio O/T is approximately 0.6 [14–17]. Similarities between crystal structures favor epitaxial growth of the γ-Ga_2O_3 thin films on sapphire substrates [18–20]. In the metastable γ-varieties of gallium oxide with defective spinel-type structure Ga^{3+} ions occupy the available cation sites per unit cell, but a small fraction of these sites remains vacant. The exact fraction of sites and whether these vacant sites are in the tetrahedral or in the octahedral sublattices depends upon the sample preparation methods and conditions.

The stoichiometric γ-Ga_2O_3 is a diamagnetic material but doping by different metals has been used to extend its functionalities for applications. Particularly, theoretical calculations and experimental data [21] reveal that strong ferromagnetic (FM) coupling between Fe ions by p – d orbital overlap of the Fe–O bond and defects, demonstrating the high-performance of γ-Ga_2O_3 as a diluted magnetic semiconductor with a Curie temperature higher than room temperature (RT). Also, Cu [18], Zn [22], Mn [19,20,23,24], and Si [25] dopants have been investigated, but room-temperature ferromagnetism (RTFM) is reported only for γ-Ga_2O_3 thin films doped with Mn and Fe. The saturation magnetic moments given in Bohr magneton unit per dopant metal in these doped γ-Ga_2O_3 thin films are $m_s = 0.42\ \mu_B$/Mn [19] and $m_s = 5.73\ \mu_B$/Fe [21], respectively.

Recently we reported the preparation of γ-Ga_2O_{3-x} ($0.4 < x < 0.6$) thin films on c-cut sapphire wafers using thermal evaporation and subsequent post-deposition thermal treatment at 600 °C under different oxygen partial pressures [26]. According to X-ray powder diffraction measurements, these Ga_2O_{3-x} thin films have cubic spinel-type structure defective but oriented with (001) crystallographic planes almost parallel with the c-cut surface of epi-polished sapphire substrates. In the present study, we report the magnetic characterization of these undoped γ-Ga_2O_3 films which ferromagnetism above RT has never been reported in the literature to our knowledge. The presence of oxygen vacancies and their interactions are directly correlated with the formation of magnetic moment and the long-range magnetic order, but these points are still not completely clear.

Otherwise, point defects are unavoidable, and they can be introduced to the material either during the fabrication or post-preparation in many ways including doping and radiation damage. Generally, the oxygen vacancies are of considerable interest because they can be closely correlated with electronic and magnetic properties in several wide-band-gap oxide nanostructures [27] and films [28], but how spin polarization caused by the presence of oxygen vacancies gives rise to long-range magnetic ordering remains a controversial research topic [29–34].

2. Experimental

A series of Ga_2O_3 thin film studied in this work were prepared using thermal evaporation on epi-polished commercial c-plane (0001)-oriented sapphire wafers (MTI Corp) using a commercial electron-beam evaporator system (Ångström engineering, evovac 046) equipped with a high precision quartz microbalance, previously calibrated by profilometry (Dektak-150). All deposition procedures were performed using a high purity gallium source (>99.9999%) with sapphire substrates maintained at room temperature by keeping specific values of oxygen partial pressure in the evaporation chamber. The oxygen partial pressure of 1 mPa was used to obtain the samples labeled as GA1 and GA2, but sample GA2 was subsequently thermal treated at 600 °C for 30 min using a dedicate high vacuum chamber with a base pressure of 10^{-5} Pa. The samples labeled as GA3 and GA4 were deposited at room temperature by keeping oxygen partial pressure values of 4 and 8 mPa, respectively. Subsequently, both samples were thermal treated at 600 °C for 30 min using the same dedicate high vacuum chamber with a base pressure of 10^{-5} Pa. All films were deposited at a fixed deposition rate of 0.14 nm/s for about 2 min resulting in 28 nm-thick oxide thin films. Details of morphology, chemical analyses, and crystal structure characterizations were published elsewhere [26].

Magnetic measurements were performed using the Magnetic Property Measurement System (MPMS®3) which combine SQUID (Quantum Design) technology with vibrating sample magnetometer using the field cooling (FC) and zero-field cooling (ZFC) protocols. The substrates are epi-polished sapphire square plates with an area of 25 mm^2 and thickness of 0.5 mm. The magnetic fields were applied parallel to the thin film plane.

3. Results and discussion

The magnetic hysteresis loops measured at RT of all studied samples are shown in Fig. 1. All the hysteresis loops measured at different temperatures are plotted after procedures for extracting diamagnetic signals of about - (15,84 ± 0,66) nemu/Oe originated from the sapphire substrates and sample holder. Clearly, all samples show soft magnetic behavior with low remanence and moderate coercivity values. The saturation magnetic fields are found close to 25 kOe at 300 K but for decreasing temperatures the saturation magnetization is attained at much higher magnetic fields. Only the sample GA1 exhibits saturation fields of about 25 kOe at all measured temperatures. The remanence ratio which is defined as saturation remanent magnetization (M_R) to saturation magnetization (M_S) is higher for samples GA1 and GA2 comparatively to the samples GA3 and GA4 across the entire range of measured temperatures.

The main magnetic details of the hysteresis loops measured for the samples are summarized in Table 1. Estimated values of the saturation magnetic moments are also given in units of Bohr magnetons per oxygen vacancy. Clearly, the introduction of oxygen vacancies would induce ferromagnetism in Ga_2O_{3x} but the magnetization is not proportional to the oxygen vacancy concentration. The two samples GA1 and GA2 with highest oxygen deficiency ($x = 0.60$ and $^{0.53,\ \text{respectively)}\ \text{show lowest}}\ \mu_{sat}$ values and larger areas of hysteresis loops comparatively with the two samples GA3 and GA4 with $x = 0.46$ and 0.42, respectively.

To better understand the magnetic behavior of the samples, magnetization measurements using field cooling (FC) and zero-field cooling (ZFC) protocols were performed using different cooling field (H_{FC}) values. The FC and ZFC magnetization curves for H_{FC} values smaller than saturation fields are shown in Fig. 2.

For $H_{FC} = 1$ kOe, the FC and ZFC curves for all samples exhibit bifurcations below 300 K. This behavior indicates the presence of magnetic irreversibility's the samples. Particularly, sample GA1 exhibit an anomalous behavior in the ZFC magnetization curve in which a broad maximum of magnetization is observed around 75 K. For $H_{FC} = 5$ kOe, ZFC and FC magnetization curves of sample GA1 also exhibit a bizarre behavior comparatively to other three samples, which only below 100 K exhibit significant bifurcations between ZFC and FC curves. Therefore, the ZFC and FC magnetization results indicate the presence of magnetic irreversibility's in the magnetization curves in all samples, but mainly in the GA1 sample, which presents a greater stoichiometric deviation and a higher concentration of defects. The presence of magnetic inhomogeneities is convincing evidence of the presence of sample regions in the form of clusters with magnetic moment arrangements along directions preferentially different from the applied magnetic field direction.

The temperature dependence of magnetization was measured for all samples using a magnetic field of 50 kOe, which is high enough to effectively saturate the magnetization of all samples. The magnetic results are shown in Fig. 3. For all samples, the saturation magnetization decreases almost linearly with increasing temperature in the temperature range between 100 K and 350 K. This result indicates an unconventional ferromagnetic-like behavior with Curie temperatures well

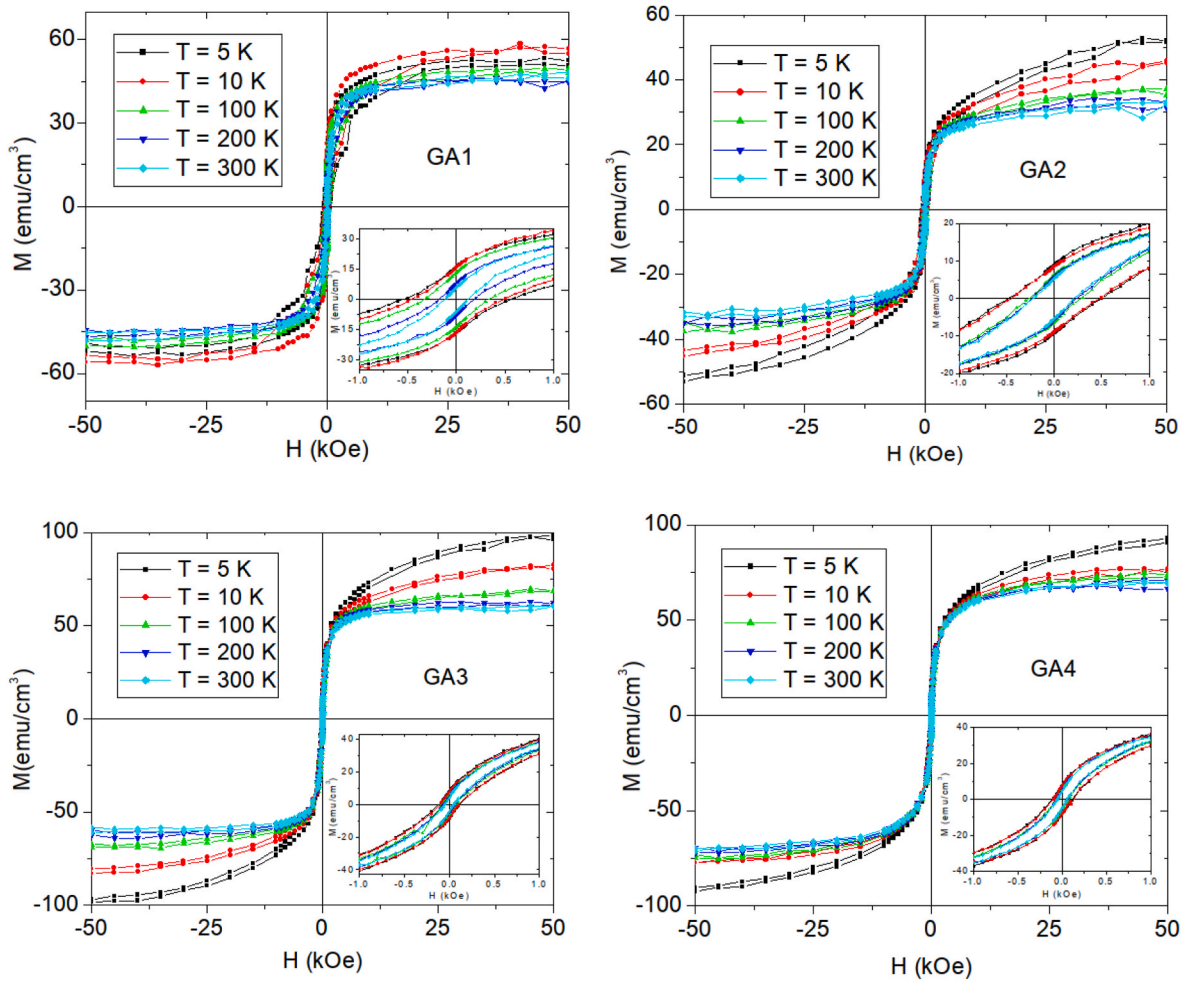

Fig. 1. Magnetic hysteresis loops measured in five different temperatures for samples GA1, GA2, GA3, and GA4. Insets show the inner part of the hysteresis loops.

Table 1
Sample identification (ID) with measured stoichiometry and their saturation magnetic moment (μ_{sat}) given in Bohr magneton (μ_B) per oxygen vacancy (VO), remanent to saturation magnetization ratio ($R = M_R/M_S$), and coercive field (Hc) values are given at 5 K and 300 K.

Sample ID-$Ga_{3-x}O_{2.40}$	μ_{sat} (μB/VO)	R ratio (%)	H_C (Oe)
GA1-$Ga_{2.40}O_{2.47}$	0.65/0.58	32/12	550/120
GA2-$Ga_{2.47}O_{2.54}$	0.74/0.43	18/20	480/220
GA3-$Ga_{2.54}O_{2.58}$	1.61/0.98	9/7	114/50
GA4-$Ga_{2.58}O_{2.58}$	1.77/1.24	8/7	110/50

above the room temperature. The GA4 and GA3 samples, which have smaller stoichiometric deviations than the GA1 and GA2 samples, exhibit greater saturation magnetizations in the studied temperature range.

In the saturation magnetization curves of all samples, it is possible to observe an increase in magnetization for temperatures below 25 K. This behavior suggests the presence of a fraction of isolated or approximately uncoupled magnetic moments in all samples that adopt the orientation of the cooling field only when thermal fluctuations are reduced at low temperatures. According to this assumption, the fraction of isolated magnetic moments in relation to the total magnetic moment would be higher in the GA3 sample. Another important result that can be extracted from the experimental data shown in Fig. 3 is that the saturation magnetizations of samples GA4 and GA3, which have smaller stoichiometric deviations, are greater than those presented by samples GA1 and GA2 with larger stoichiometric deviations. Therefore, the saturation magnetization is not directly proportional to the oxygen stoichiometry deviations of the films. In fact, the larger the stoichiometric deviation is, the smaller the saturation magnetization observed at low temperature.

Without evidence of any contaminants in the samples, then the ferromagnetic-like behavior in the γ-Ga_2O_3 thin films presumably comes from the oxygen vacancies and defects, which quantities must be enough to create an interconnected network to settle down a long-range magnetic ordering.

An estimate of the number of oxygen atoms in the samples can be obtained using the crystal cell parameters for γ-Ga_2O_3 with cubic spinel structure and the calculated density of 5.94 g/cm^3, which is commonly higher than the measured density values [16]. To maintain the overall measured stoichiometric deviations given in Table 1, it is necessary that all four Ga sites are fully occupied, and the oxygen sites are partially occupied in the ideal cubic spinel structure. Taking the sample volume corresponding to the area multiplied by the thickness of the thin films and the volume of a unit cell occupied by a γ-Ga_2O_3 formula unit (f.u.) we can estimate the number of oxygen vacancies and the mean values of magnetic moment per vacancy. The μ_{sat} values found for samples GA4 and GA3 are more than twice the values for samples GA1 and GA2 whether at 5 K or RT. It should be emphasized that the procedure used to estimate the saturated magnetic moments per oxygen vacancies (given in Table 1) only leads to net values of total magnetic moment that do not consider eventual non-collinear or antiparallel arrangements of magnetic moments in the oxygen vacancy network.

To activate the magnetism potential in various otherwise diamagnetic oxides, the most common strategy is to incorporate the dopants

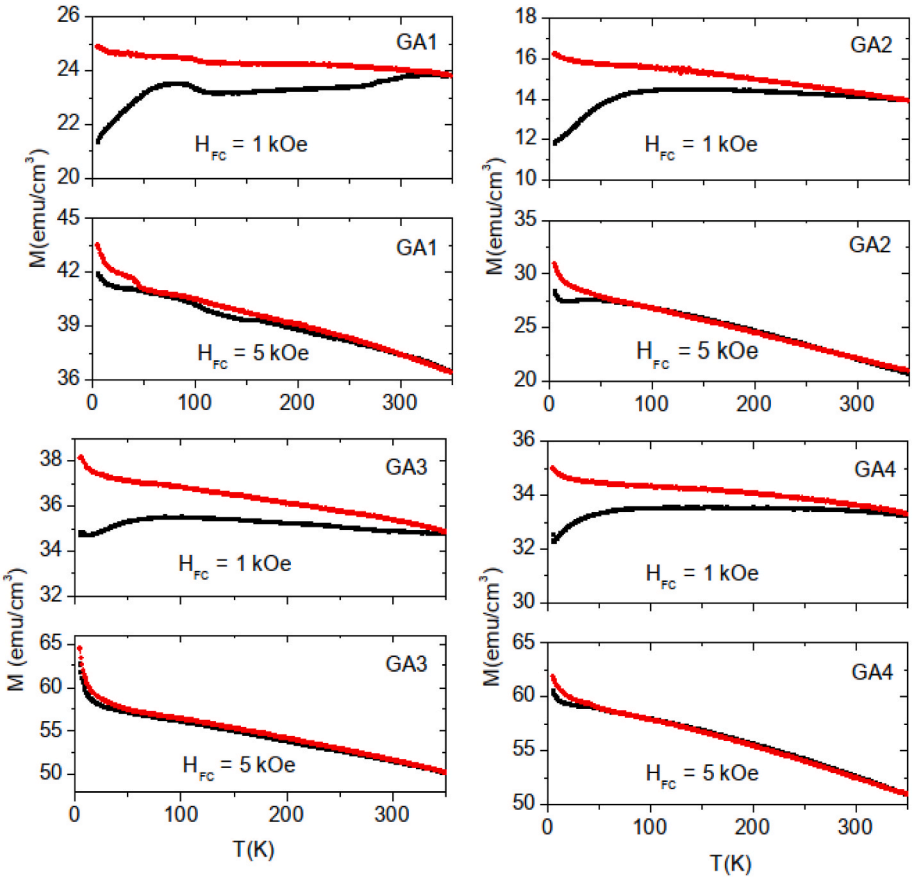

Fig. 2. Measurements of the magnetizations using ZFC (black squares) and FC (red dots) protocols using field cooling (HFC) values of 1 kOe and 5 kOe from samples GA1, GA2, GA3 and GA4. Diamagnetic contributions were extracted from the magnetization curves. (For interpretation of the references to colour in this figure legend, the reader is referred to the Web version of this article.)

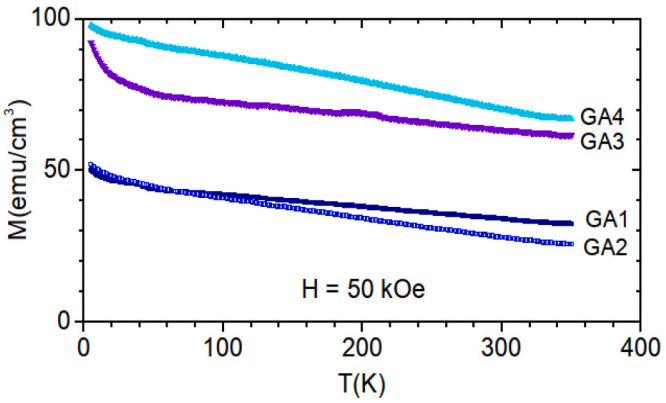

Fig. 3. Temperature dependence of the saturation magnetization of the thin films for a saturation magnetic field of 50 kOe.

that lead to so-called dilute magnetic oxides [35]. To the best of our knowledge, however, there are only two experimental works reporting RTFM in doped γ-Ga_2O_3. RTFM was observed in Mn-doped γ-Ga_2O_3 grown on c-cut sapphire substrate using pulsed-laser deposition technique [19] and Fe-doped γ-Ga_2O_3 grown on (0001) sapphire substrates by the laser molecular beam epitaxy technique [21].

RTFM behavior reported in Mn-doped γ-Ga_2O_3 thin films reveal RT saturation magnetic moments of 0.42 μ_B/Mn [19] and first-principles calculations reveal that the Mn atoms are preferably located at tetrahedrally coordinated Ga sites with the valence of +2, whereas the cation vacancies were energetically favorable at the octahedral sites [36].

For Fe-doped γ-Ga_2O_3 thin films deposited on sapphire substrates show saturation magnetic moment at room temperature as high as 5.73 μ_B/Fe [21]. The first principles calculations performed reveal that the main source of RTFM can be ascribed to the strong ferromagnetic coupling between Fe ions, p–d orbital overlap of the Fe–O bond and defects. Among defects, there are cation (gallium) vacancies and mainly oxygen vacancies. Therefore, the dislocation of the Fe^{3+} and Fe^{2+} ions as well as oxygen vacancies can also induce interactions between the magnetic dopants leading to the local electric charge distributions with a certain spin polarization.

Comparatively, non-doped γ-Ga_2O_3 thin films rich in oxygen vacancies like the samples studied in the present work exhibit moderately high magnetic moments per oxygen vacancy and strong magnetic irreversibility's, as indicated by the magnetic measurements using FC/ZFC protocols. It is worth to remember, however, that measured saturation magnetic moments per formula unit can be higher than the net estimated values, since partially compensated arrangements of magnetic moments could remain misoriented relatively to the applied magnetic field orientation even at the available maximum fields of 60 kOe.

The origin of the observed magnetism it is still not completely understood. First-principal theoretical calculations were performed for an ideal cubic γ-phase of $Ga_{24}O_{32}$ supercell [21]. In this case, the crystallographic unit cell contains 32 cubic-close-packed oxygen ions (eight chemical formula units), giving rise to hypothetical and fully occupied crystal structure with 16 octahedrons (O) and 8 tetrahedrons (T) in the supercell with two nonequivalent Ga sites, Ga_O and Ga_T, which are octahedrally and tetrahedrally coordinated, respectively. The calculated total and local density of states of γ-$Ga_{24}O_{32}$ supercell show that the spin-up and spin-down orbitals are symmetrical. Either the Ga_O, Ga_T and

O sites all have a spin magnetic moment of zero, indicating that the fully occupied γ-$Ga_{24}O_{32}$ structure has a non-magnetic structure, i.e., it is diamagnetic material.

To explain the origin of the robust ferromagnetic-like behavior observed in oxygen-deficient γ-Ga_2O_3 films, we propose an explanation made on the basis of limited evidence as a starting point for further investigation the following mechanism. Nonmagnetic investigations of the oxygen vacancies have undoubtedly demonstrated that the charge state of the vacancy has pronounced effects on its electronic and structural properties of γ-Ga_2O_3 [12,13]. Clustering of oxygen vacancies is very likely, and it would result localized moment around vacant sites in the same context of dilute magnetic oxides. Therefore, defect-induced localized magnetic moments can form bound magnetic polarons [37] with appreciable magnetic moments and thermal stability as robust as the electronic structure [38] as long as the oxygen vacancy migration mechanisms are not activated [39]. Furthermore, both the presence of two non-equivalent Ga sites with octahedral and tetrahedral coordination, as well as the local stress created in γ-Ga_2O_3 accommodating oxygen stoichiometry changes, allows us to predict the possibility of forming arrangements of magnetic moments that are not necessarily collinear with each other. In fact, if oxygen vacancies and defects are responsible for the formation of magnetic moments with unusual magnetic coupling, even a small disorder in the magnetic moment lattice can possibly induce a non-uniform distribution of magnetic moments with different magnitudes and orientations. This assumption may explain why saturation magnetization is not directly proportional to the oxygen deficiency of each sample, as shown in Table 1.

In fact, defect-induced magnetism in transition metal oxides is predicted by a number of models [40]. Beyond the type of the magnetic interactions and the establishment of the long-range magnetic coupling between two magnetic centers, the approaches consider the rehybridization of the atomic orbitals associated with the defects themselves (such as vacancies) and those of the surrounding the defect ligands which have local character depending on inter- and intra-atomic charge redistributions. These features are used to explain defect-induced ferromagnetic and antiferromagnetic coupling in co-doped transition metal oxides because it facilitates the development of delocalized spin-polarized molecular orbitals over a more extended range [41]. The presence of octahedrally and tetrahedrally coordinated defective sites in γ-phase of Ga_2O_{3-x} films with cubic spinel structure is often assigned to mixtures of more than one type of both octahedral and tetrahedral Ga sites of nonideal local symmetry [15]. It is not surprising, therefore, that the reduction in saturation magnetization with increasing sample oxygen deficiency occurs as a consequence of the conflicting superposition of extended magnetic couplings.

The present experimental study on the undoped γ-Ga_2O_3 samples rich in oxygen vacancies clearly demonstrate the possibility to induce ferromagnetic-like behavior at room temperature with formation of moderately high saturation magnetic moments values. Despite RTFM has been observed in several undoped semiconducting and insulating oxides, the present observation in γ- Ga_2O_3 extends the functionalities of this interesting material to the magnetism area.

4. Final remarks

Despite recent advances in the growth of gallium oxide thin films, which are rapidly emerging as a material of choice for many applications, current Ga_2O_3 technology is not yet mature for commercial use. This work highlights the role of polymorphism and optimization of Ga_2O_3 performance in the γ phase by controlling the defect structure. The present results indicate that the exploration of the conditions of synthesis and composition is a rich field for future research. Specifically, the demonstration of an ease way to induce ferromagnetism at room temperature in γ-Ga_2O_3 films adds an important multifunctionality which opens possibilities to explore spintronics and optospintonics applications.

Declaration of competing interest

The authors declare that they have no known competing financial interests or personal relationships that could have appeared to influence the work reported in this paper.

Acknowledgments

The authors thank the Brazilian agencies CAPES and CNPq for the partial financial support for the development of research activities, as well as the support of the National Nanotechnology Laboratory (LNNano) in the open national facilities operated by the Brazilian Center for Research in Energy and Materials (CNPEM) and FAPESP 09/54082-2 e 13/07296-2.

References

[1] B.R. Tak, S. Kumar, A.K. Kapoor, D. Wang, X. Li, H. Sun, R. Singh, Recent advances in the growth of gallium oxide thin films employing various growth techniques - a review, J. Phys. Appl. Phys. 54 (2021) 22, https://doi.org/10.1088/1361-6463/ac1af2.

[2] S. Penner, C. Zhuo, R. Thalinger, M. Grünbacher, C. Hejny, S. Vanicek, M. Noisternig, Physico- chemical properties of unusual Ga2O3 polymorphs, Monatshefte Chemie. 147 (2016) 289–300, https://doi.org/10.1007/s00706-015-1628-z.

[3] R. Roy, V.G. Hill, E.F. Osborn, Polymorphism of Ga2O3 and the system Ga2O3-H2O, J. Am. Chem. Soc. 74 (1952) 719–722, https://doi.org/10.1021/ja01123a039.

[4] S.I. Stepanov, V.I. Nikolaev, V.E. Bougrov, A.E. Romanov, Gallium oxide: properties and applica a review, Rev. Adv. Mater. Sci. 44 (2016) 63–86.

[5] S. Yoshioka, H. Hayashi, A. Kuwabara, F. Oba, K. Matsunaga, I. Tanaka, Structures and energetics of Ga2O3 polymorphs, J. Phys. Condens. Matter 19 (2007) 346211, https://doi.org/10.1088/0953-8984/19/34/346211.

[6] X. Zhang, Z. Zhang, H. Huang, Y. Wang, N. Tong, J. Lin, D. Liu, X. Wang, Oxygen vacancy modulation of two-dimensional γ-Ga2O3 nanosheets as efficient catalysts for photocatalytic hydrogen evolution, Nanoscale 10 (2018) 21509–21517, https://doi.org/10.1039/c8nr07186a.

[7] S.S. Farvid, T. Wang, P.v. Radovanovic, Colloidal gallium indium oxide nanocrystals: a multifunctional light-emitting phosphor broadly tunable by Alloy composition, J. Am. Chem. Soc. 133 (2011) 6711–6719, https://doi.org/10.1021/ja111514u.

[8] S. Jin, X. Wang, X. Wang, M. Ju, S. Shen, W. Liang, Y. Zhao, Z. Feng, H.Y. Playford, R.I. Walton, C. Li, The effect of phase junction structure on the photocatalytic performance in overall water splitting: Ga2O3 photocatalyst as an example, J. Phys. Chem. C 119 (2015) 18221–18228, https://doi.org/10.1021/acs.jpcc.5b04092.

[9] T. Chen, K. Tang, γ- Ga2O3 quantum dots with visible blue-green light emission property, Appl. Phys. Lett. 90 (2007), 053104, https://doi.org/10.1063/1.2437110.

[10] T. Wang, S.S. Farvid, M. Abulikemu, P.v. Radovanovic, Size-tunable phosphorescence in colloidal metastable γ-Ga 2O3 nanocrystals, J. Am. Chem. Soc. 132 (2010) 9250–9252, https://doi.org/10.1021/ja101333h.

[11] A. Singhal, I. Lieberwirth, Non-aqueous synthesis of blue light emitting γ-Ga2O3 and c-In2O3 nanostructures from their ethylene glycolate precursors, Mater. Lett. 161 (2015) 112–116, https://doi.org/10.1016/j.matlet.2015.07.130.

[12] T. Wang, P. v. Radovanovic, in situ enhancement of the blue photoluminescence of colloidal Ga 2O3 nanocrystals by promotion of defect formation in reducing conditions, Chem. Commun. 47 (2011) 7161–7163, https://doi.org/10.1039/c1cc11957e.

[13] V. Ghodsi, S. Jin, J.C. Byers, Y. Pan, P.v. Radovanovic, Anomalous photocatalytic activity of nanocrystalline γ-phase Ga2O3 enabled by long-lived defect trap states, J. Phys. Chem. C 121 (2017) 9433–9441, https://doi.org/10.1021/acs.jpcc.7b02275.

[14] K. Nishi, K.I. Shimizu, M. Takamatsu, H. Yoshida, A. Satsuma, T. Tanaka, S. Yoshida, T. Hattori, Deconvolution analysis of Ga K-Edge XANES for quantification of gallium coordinations in oxide environments, J. Phys. Chem. B 102 (1998) 10190–10195, https://doi.org/10.1021/jp982704p.

[15] H.Y. Playford, A.C. Hannon, M.G. Tucker, D.M. Dawson, S.E. Ashbrook, R. J. Kastiban, J. Sloan, R.I. Walton, Characterization of structural disorder in γ-Ga2O3, J. Phys. Chem. C 118 (2014) 16188–16198, https://doi.org/10.1021/jp5033806.

[16] H.Y. Playford, A.C. Hannon, E.R. Barney, R.I. Walton, Structures of uncharacterised polymorphs of gallium oxide from total neutron diffraction, Chem. Eur J. 19 (2013) 2803–2813, https://doi.org/10.1002/chem.201203359.

[17] C. Otero Areán, M. Rodríguez Delgado, V. Montouillout, D. Massiot, Synthesis and characterization of spinel-type gallia-alumina solid solutions, Z. Anorg. Allg. Chem. 631 (2005) 2121–2126, https://doi.org/10.1002/zaac.200570027.

[18] Q. Liu, D. Guo, K. Chen, Y. Su, S. Wang, P. Li, W. Tang, Stabilizing the metastable γ phase in Ga2O3 thin films by Cu doping, J. Alloys Compd. 731 (2018) 1225–1229, https://doi.org/10.1016/j.jallcom.2017.10.162.

[19] H. Hayashi, R. Huang, H. Ikeno, F. Oba, S. Yoshioka, I. Tanaka, S. Sonoda, Room temperature ferromagnetism in Mn-doped γ- Ga2O 3 with spinel structure, Appl. Phys. Lett. 89 (2006) 181903, https://doi.org/10.1063/1.2369541.
[20] R. Huang, H. Hayashi, F. Oba, I. Tanaka, Microstructure of Mn-doped γ-Ga2O3 epitaxial film on sapphire (0001) with room temperature ferromagnetism, J. Appl. Phys. 101 (2007), 063526, https://doi.org/10.1063/1.2713349.
[21] Y. Huang, A. Gao, D. Guo, X. Lu, X. Zhang, Y. Huang, J. Yu, S. Li, P. Li, W. Tang, Fe doping- stabilized γ-Ga2O3 thin films with a high room temperature saturation magnetic moment, J. Mater. Chem. C 8 (2020) 536–542, https://doi.org/10.1039/c9tc05823k.
[22] V. Vasanthi, M. Kottaisamy, V. Ramakrishnan, Near UV excitable warm white light emitting Zn doped γ-Ga2O3 nanoparticles for phosphor-converted white light emitting diode, Ceram. Int. 45 (2019) 2079–2087, https://doi.org/10.1016/j.ceramint.2018.10.111.
[23] H. Hayashi, R. Huang, F. Oba, T. Hirayama, I. Tanaka, Atomistic structure and energetics of interface between Mn-doped γ-Ga2O3 and MgAl2O4, J. Mater. Sci. 46 (2011) 4169–4175, https://doi.org/10.1007/s10853-011-5313-2.
[24] H. Hayashi, R. Huang, F. Oba, T. Hirayama, I. Tanaka, Epitaxial growth of Mn-doped γ-Ga2O3 on spinel substrate, J. Mater. Res. 26 (2011) 578–583, https://doi.org/10.1557/jmr.2010.32.
[25] T. Oshima, K. Matsuyama, K. Yoshimatsu, A. Ohtomo, Conducting Si-doped γ-Ga2O3 epitaxial films grown by pulsed-laser deposition, J. Cryst. Growth 421 (2015) 23–26, https://doi.org/10.1016/j.jcrysgro.2015.04.011.
[26] A. Pichorim, D. da S. Costa, I.T. Neckel, D.H. Mosca, Non-stoichiometric Gallium oxide with cubic structure directly integrated to c-cut sapphire, Mater. Sci. Semicond. Process. 139 (2022) 106349, https://doi.org/10.1016/j.mssp.2021.106349.
[27] A. Sundaresan, R. Bhargavi, N. Rangarajan, U. Siddesh, C.N.R. Rao, Ferromagnetism as a universal feature of nanoparticles of the otherwise nonmagnetic oxides, Phys. Rev. B Condens. Matter 74 (2006) 161306, https://doi.org/10.1103/PhysRevB.74.161306.
[28] N.H. Hong, J. Sakai, N. Poirot, V. Brizé, Room-temperature ferromagnetism observed in undoped semiconducting and insulating oxide thin films, Phys. Rev. B Condens. Matter 73 (2006) 132404, https://doi.org/10.1103/PhysRevB.73.132404.
[29] V. Fernandes, R.J.O. Mossanek, P. Schio, J.J. Klein, A.J.A. de Oliveira, W.A. Ortiz, N. Mattoso, J. Varalda, W.H. Schreiner, M. Abbate, D.H. Mosca, Dilute-defect magnetism: origin of magnetism in nanocrystalline CeO2, Phys. Rev. B Condens. Matter 80 (2009), 035202, https://doi.org/10.1103/PhysRevB.80.035202.
[30] S. Mal, S. Nori, C. Jin, J. Narayan, S. Nellutla, A.I. Smirnov, J.T. Prater, Reversible room temperature ferromagnetism in undoped zinc oxide: correlation between defects and physical properties, J. Appl. Phys. 108 (2010), 073510, https://doi.org/10.1063/1.3491037.
[31] B. Santara, P.K. Giri, K. Imakita, M. Fujii, Evidence of oxygen vacancy induced room temperature ferromagnetism in solvothermally synthesized undoped TiO2 nanoribbons, Nanoscale 5 (2013) 5476–5488, https://doi.org/10.1039/c3nr00799e.
[32] B. Qi, S. Ólafsson, H.P. Gíslason, Vacancy defect-induced d0 ferromagnetism in undoped ZnO nanostructures: controversial origin and challenges, Prog. Mater. Sci. 90 (2017) 45–74, https://doi.org/10.1016/j.pmatsci.2017.07.002.
[33] H. Zhang, W. Li, G. Qin, H. Ruan, D. Wang, J. Wang, C. Kong, F. Wu, L. Fang, Surface ferromagnetism in ZnO single crystal, Solid State Commun. 292 (2019) 36–39, https://doi.org/10.1016/j.ssc.2019.01.021.
[34] S.M. Yakout, Room temperature ferromagnetism: nonmagnetic semiconductor oxides and nonmagnetic dopants, J. Electron. Mater. 50 (2021), https://doi.org/10.1007/s11664-021-08777-z, 1922–1941.
[35] W. Prellier, A. Fouchet, B. Mercey, Oxide-diluted magnetic semiconductors: a review of the experimental status, J. Phys. Condens. Matter 15 (2003) 1583–1601, https://doi.org/10.1088/0953-8984/15/37/R01.
[36] H. Hayashi, R. Huang, F. Oba, T. Hirayama, I. Tanaka, Site preference of cation vacancies in Mn- doped Ga2O3 with defective spinel structure, Appl. Phys. Lett. 101 (2012) 241906, https://doi.org/10.1063/1.4770363.
[37] J.M.D. Coey, M. Venkatesan, C.B. Fitzgerald, Donor impurity band exchange in dilute ferromagnetic oxides, Nat. Mater. 4 (2005) 173–179, https://doi.org/10.1038/nmat1310.
[38] O.O. Brovko, E. Tosatti, Controlling the magnetism of oxygen surface vacancies in SrTiO3 through charging, Phys. Rev. Mater. 1 (2017), 044405, https://doi.org/10.1103/PhysRevMaterials.1.044405.
[39] J. Varalda, C.A. Dartora, P.C. de Camargo, A.J.A. de Oliveira, D.H. Mosca, Oxygen diffusion and vacancy migration thermally-activated govern high-temperature magnetism in ceria, Sci. Rep. 9 (2019) 1–9, https://doi.org/10.1038/s41598-019-41157-6.
[40] A.N. Andriotis, M. Menon, Codoping induced enhanced ferromagnetism in diluted magnetic semiconductors, J. Phys. Condens. Matter 33 (2011) 393002. https://orcid.org/0000-0002-8283- 138X.
[41] A.N. Andriotis, M. Menon, Defect-induced magnetism: codoping and a prescription for enhanced magnetism, Phys. Rev. B 87 (2013) 155309, https://doi.org/10.1103/PhysRevB.87.155309.